Liquid metals as a divertor plasma facing material explored using the Pilot-PSI and Magnum-PSI linear devices

T.W.Morgan[1], P. Rindt[2], G.G. van Eden[1], V. Kvon[1], M.A. Jaworksi[3] and N.J. Lopes Cardozo[2]

[1] DIFFER – Dutch Institute for Fundamental Energy Research, De Zaale 20, 5612 AJ Eindhoven, The Netherlands

[2] Department of Applied Physics, Eindhoven University of Technology, Eindhoven, The Netherlands

[3] Princeton Plasma Physics Laboratory, Princeton NJ, USA

Abstract

For DEMO and beyond liquid metal plasma facing components are considered due to their resilience to erosion through flowed replacement, potential for cooling beyond conduction and inherent immunity to many of the issues of neutron loading compared to solid materials. The development curve of liquid metals is behind that of e.g. tungsten however and tokamak-based research is currently somewhat limited in scope. Therefore investigation in linear plasma devices can provide faster progress under controlled and well-diagnosed conditions in assessing many of the issues surrounding the use of liquid metals. The linear plasma devices Magnum-PSI and Pilot-PSI are capable of producing DEMO relevant plasma fluxes which well replicate expected divertor conditions, and the exploration of physics issues for tin (Sn) and lithium (Li) such as vapour-shielding, erosion under high particle flux loading and overall power handing are reviewed here. A deeper understanding of erosion and deposition through this work indicates that stannane formation may play an important role in enhancing Sn erosion, while on the other hand the strong hydrogen isotope affinity reduces the evaporation rate and sputtering yields for Li. In combination with the strong re-deposition rates which have been observed under this type of high density plasma this implies an increase in the operational temperature range, implying a power handling range of 20-25 MW m^{-2} for Sn and up to 12.5 MW m^{-2} for Li could be achieved. Vapour shielding may be expected to act as a self-protection mechanism in reducing the heat load to the substrate for off-normal events in the case of Sn, but may potentially be a continual mode of operation for Li.

1. Introduction

Economical electricity production via magnetic confinement fusion requires the successful development and deployment of both ITER [1][2] and DEMO [3]. The Eurofusion roadmap [4] identified that "a reliable solution to the problem of heat exhaust is probably the main challenge towards the realisation of magnetic confinement fusion", while within that challenge the wall components in the divertor are the limiting factor which define the costs, lifetime and viability of the exhaust system.

Given the choice of tungsten for the plasma facing material (PFM) in the ITER divertor, it is worth reviewing firstly the potential difficulties and concerns in using a similar divertor plasma facing component (PFC) design for DEMO as for ITER, and which therefore motivates the search for an alternative PFM.

In going from ITER to DEMO two properties in particular increase by around an order of magnitude. The first is the fusion power generated, while the second is the neutron loading to the walls [5], as a consequence of the first, combined with the much higher duty cycle [6]. The higher fusion power implies that a much larger fraction of the stored energy must be radiated in the core [7], while ensuring the power crossing the separatrix lies above the H-L power

1

threshold [8], [9]. This in turn indicates a much smaller margin of error to avoid exceedingly high powers reaching the divertor which would quickly damage components. Furthermore the higher neutron loading implies a continual level of damage creation and transmutation [10] which makes resilience against neutron loading of increased importance.

Tungsten has many advantages which have led to its selection for ITER, such as high melting point, high thermal conductivity, low solubility and retention of tritium, high strength and low sputtering rate [11]. Despite this latter point however a 5 mm thick W armour is not projected to have a lifetime of longer than 2 years in DEMO [12]. In other words the erosion rate sets a minimum thickness level for tungsten which then limits the heat load that can be conducted through the block to the cooling water.

Secondly tungsten is a highly brittle material which is susceptible to thermal shock and fatigue [13]. This can arise both from transient loading such as ELMs, slow transients due to temporary re-attachment as well as cyclical loading should DEMO operate in pulsed mode as is currently expected [12]. Such cyclical loading can give rise to both so-called macro-cracking [14] as well as microcracks at the surface [13][15][16]. The evidence so far shows a progressive degradation of the material may be expected under cyclical loading [15][17], and that over long periods and large cycle numbers even initially benign transient loading may lead to deterioration of the material [18][19]. This therefore implies that large cycle number loading such as ELMs may have to be entirely eliminated in DEMO, which has implications for operating in H-mode, or that improvements in PFCs which could better tolerate transient loading must be achieved.

Thirdly off-normal events such as vertical displacement events, disruptions [20] or unmitigated ELMs [21] would be expected to melt a tungsten divertor surface. This therefore leads to irreversible damage which may require replacement of the entire component. This would be costly and time consuming, reducing the competitiveness and reliability of any future fusion power plant.

Lastly neutron loading will be at a much higher level in DEMO than in ITER, at an order of 1-9 dpa per full power year in the divertor [5] compared to 0.7 dpa over the ITER divertor lifetime in the DT phase [22]. This will lead to defect creation as well as transmutation to rhenium and osmium [10], as well as hydrogen and helium generation which may be expected to reduce the thermal diffusivity [23] and increase hardness and DBTT as well as reduce the recrystallization threshold [24]. The result would be a progressive decrease in the operational temperature window and thus power handling capability over time, as well as increased susceptibility to cracking through increased brittleness.

The use of a liquid metal (LM) as the PFM has several attractive properties which would be expected to ameliorate at least partially many of these concerns. In the case of erosion a molten material can resupply any eroded areas, eliminating this as a lifetime concern. This in turn permits a thinner component to be designed which could exhaust higher levels of power than a thicker W component. Power limits for Sn based PFCs of up to 20-25 MW m^{-2} have been estimated [25][26]. Secondly a liquid surface by its nature cannot crack, and potentially components could be designed which are better able to withstand transient loading in such a case. Under off-normal loading, on the one hand an initially molten material can be replaced, while furthermore vapour shielding through strong evaporation may be expected to help shield the surface and reduce the heat loading to the substrate [27]. Therefore in the case of accidental excessive heat loading the liquid PFC will act as a negative feedback mechanism on the plasma. A liquid metal based PFM may therefore be able to recover from such events without component replacement. Finally neutron loading cannot lead to defect creation in a liquid, while any transmuted products may be replaced by the influx of new material, preventing any gradual degradation in thermophysical properties. Thus, while the underlying substrate will be influenced by neutron loading, the plasma surface interaction is isolated from this effect.

Overall a LM based PFC may be a more forgiving component in tolerating power of similar or higher heat loads as well as off-normal and transient loading. As a final point, innovative designs involving liquid metals also offer the possibility of cooling beyond only conduction to a coolant, e.g. through evaporative cooling [28], vapour shielding [29], convection [30][31] or a combination [32]. This might greatly improve power handling capabilities, though such designs are typically at a conceptual level currently.

The much greater body of knowledge on the performance of W PFCs, their higher level of technological maturity as well as the greater simplicity in using a solid tungsten surface compared to a liquid makes it the leading candidate for DEMO. At the present time liquid metal based PFCs still have many potential issues in terms of engineering design, operational safety limitations or other limits such as for fuel retention which must still be fully addressed. However if ITER's results are unfavourable in extrapolating a W-based PFC to DEMO no substitute PFC option exists. It is therefore imperative to develop at least one LM based PFC design to a sufficiently advanced level in time to be considered for the design of DEMO as a viable alternative. Even beyond DEMO liquid metals may prove a more desirable and economical choice for PFC in fusion power plant and thus their development should be urgently pursued.

In such an effort linear plasma devices can play a crucial role. Such machines are simpler to operate than tokamaks and give very good diagnostic access, while also being themselves simpler to diagnose. They also can offer much greater flexibility in exchanging test samples for basic physics studies as well as PFC prototypes in a way that is challenging in a tokamak environment. In the case of Magnum-PSI [33], [34] and Pilot-PSI [35], [36] these devices can also achieve plasma conditions and heat and particle fluxes which closely replicate the conditions expected close to the divertor strikepoints in ITER and DEMO, making them excellent test-beds in studying the performance of liquid metals under realistic loading conditions. These abilities are therefore complimentary to studies in confinement devices where the complex interaction between wall, edge and core plasma can be studied, for example in terms of material migration, core contamination and global fuel retention. This paper will provide an overview of recent work carried out in these linear plasma devices in studying liquid metals on the topics of erosion and power handling studies and show how these fit within the context of worldwide research on this topic. The discussion will also identify the areas where linear machines can make significant contributions in the near future to developing a mature LM based PFC for DEMO.

2. Results and discussion

2.1 Material selection and the Capillary Porous Structure concept

For liquid metal candidates the main considerations are the melting and boiling points, their abundance and cost as well as their thermal conductivity and chemical compatibility with substrate materials and plasma constituents. The APEX studies identified Li or Sn-Li alloy, or a molten salt (FLIBE) [37] while more recently Sn, Ga and Al were proposed [25]. FLIBE has a very low thermal conductivity (1 W m^{-1} K^{-1}) [37], Ga a high chemical reactivity with many potential substrates [38] and Al has a long lived reactivity [39] which makes these options less attractive. The work described here has mostly therefore concentrated on studying Li and Sn.

Li has a low melting point (180.5 °C) and is low-Z, permitting a relatively high concentration in the core plasma (section 2.2). It is also well documented that improvements in plasma performance due to wall conditioning and Z_{eff} reduction are observed with Li use in tokamaks [40][41][42][43]. However in DEMO where first wall temperatures are expected to be high [44] the wall pumping effect may be absent, so it is unclear if such benefits will extrapolate. Furthermore Li has a high affinity for H-isotopes and can form hydrides up to a 1:1

stoichometric ratio [45]. Therefore tritium retention is a concern which must be clearly dealt with to avoid this being a showstopper and appears to require a temperature above 500-550 °C to avoid gas phase absorption in the divertor [46]. Li also reacts with water effusively giving off H_2 exothermally which can be a safety risk for water cooled systems. Lastly it has a relatively high vapour pressure [47] and therefore a relatively narrow temperature window for operation would be expected.

For Sn its concerns are similar to W, in that it is a high-Z metal, and therefore only a small concentration in the plasma core is tolerable. Its sputtering and evaporation rates are higher than W so an improved power handling and life-time performance are desirable to be competitive. Little work on D retention has been carried out under plasma exposure but retention rates measured in ISTTOK indicate retention is very low [48]. The operational temperature window may also be expected to be wider for Sn than Li due to its lower vapour pressure [47] and similar melting point (231.9 °C).

Sn-Li alloys have in recent times been more seriously reconsidered as potentially offering the best of both worlds, e.g. a $\sim 10^3$ lower evaporation pressure than pure Li [49], while segregation of Li to the surface would mean lower Sn sputtering than pure Sn [50]. The recent results at the ISTTOK tokamak also indicate a deuterium retention rate similar to Sn [48] but more research is required in the future on this material and it was not included in the present work.

One significant challenge for the use of an electrically conductive liquid metal in an environment of high magnetic and electric fields is MHD forces which can destabilize the liquid surface. For a free surface such forces can lead to Rayleigh-Taylor or Kelvin-Helmholtz instabilities for example [51]–[53], potentially driving droplet formation which would lead to strong erosion and a disruption [54]. To prevent this a system of small pores such as a mesh or porous solid can be used such that the liquid is stabilized by surface tension when wetted to the substrate. Calculations and experiments show that pore sizes of $<\sim 50$ μm are typically able to stabilize against such forces [26], [53]. The liquid surface is replenished by capillary flow through the pores as it is eroded, thus requiring typically only a small material flow. This capillary porous structure (CPS) concept [55] creates a simple and solid-like test target and was used in all work described here with the exception of [56] where a more advanced concept was investigated.

2.2 Erosion

As with all wall materials impurity levels in the core plasma set limits on what net impurity flux from the divertor is acceptable to ensure fusion power output is not significantly affected. For Li fuel dilution would be the main limitation [57], while for Sn radiation losses through line radiation and Bremsstrahlung would be the limiting factor, similar to W [58]. The relationship between core impurity concentration and wall erosion rate is complex but an approximation is to relate the tolerable core impurity concentration $f = n_{imp}/n_e$ to the impurity influx rate

$$\langle \Gamma_{imp} \rangle = \frac{fV\langle n_e \rangle}{A_{div}\tau_p} \tag{1}$$

where V is the plasma volume, $\langle n_e \rangle$ the average electron density, A_{div} the divertor area and τ_p the particle confinement time. Taking realistic numbers for DEMO [3][1] and tolerable fractions from [59] would give results of order for Li $\langle \Gamma_{Li} \rangle \sim 1 \times 10^{21}$ m^{-2} s^{-1} and for Sn $\langle \Gamma_{Sn} \rangle \sim 5 \times 10^{18}$ m^{-2} s^{-1}.

Material erosion due to plasma exposure is generally considered as a combination of physical sputtering and evaporation. Many experiments have reported a temperature dependent sputtering phenomenon (so called Temperature Enhanced Sputtering or TES) for a variety of

plasma facing materials including C [60], Be and molten Li [61] and Ga [62], where erosion is observed to increase with temperature under sputtering by ions but at temperatures well below where evaporation is expected to be significant. For Sn only a limited data set previously existed [63], [64], and only using high energy (keV) ions, thus it was chosen to also study this for molten Sn confined using CPS under more relevant plasma exposure conditions using H, He or Ar plasmas in Pilot-PSI [65].
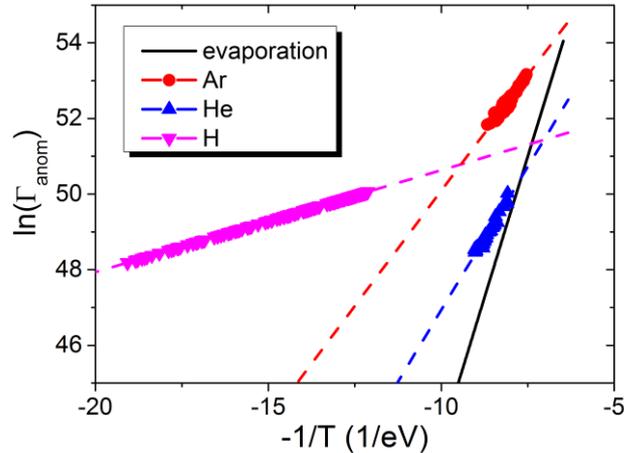

Figure 1: Temperature dependence of the anomalous sputtering flux of Sn under Ar, He or H loading in Pilot-PSI (based on data from [65]). The Arrhenius-like behaviour is similar for Ar and He despite quite different erosion fluxes but is very different for H implying a different process is responsible for the erosion flux.

Roth and Möller proposed a model [60] expanded by Doerner et al [61], [66] based on adatom formation at the surface due to sputtering, followed by sublimation of the adatoms. In such a case the particles are more weakly bound than the normal surface binding energy and so evaporation-like behaviour occurs at lower temperatures than would be expected. For Ar and He the results are comparable to those for other materials with an effective surface binding energy of E_{eff} = 1.22 eV and E_{eff} = 1.50 eV respectively compared to E_{SBE} = 3.08 eV for Sn [67]. Similar ratios are seen for D sputtering on Be (E_{eff} = 2 eV compared to E_{SBE} = 3.41 eV) and molten Li (E_{eff} = 1.1 eV compared to E_{SBE} = 1.67 eV) [61] which indicates a similar process occurs in all cases. A different behaviour is observed however for H interaction with Sn, where an increasing signal is observed with temperature at much lower temperatures than in other cases [65]. Here the effective energy is only E_{eff} = 0.27 eV which indicates a different type of thermally activated process is likely responsible (Figure 1). We proposed that stannane (SnH_4) formation may account for such an effect [65]. It is known [68] that gaseous tin hydrides can form in the presence of hydrogen radicals which would support this. On the other hand stannane thermally decomposes in gas phase above 25 °C [69] and quickly decomposes on a Sn surface at even lower temperatures [70], [71], which would imply that net erosion may be negligible if it quickly is redeposited. The implications for Sn use as a PFM however requires more systematic study to understand whether this chemical etching process is significant as a limiting factor in the use of Sn. It seems likely that at elevated temperatures evaporation would still dominate and so for power handling analysis this effect is neglected for now.

For Li there is a strong affinity between H and Li to form a solid hydride, LiH, rather than a volatile compound [45]. Up to a 1:1 Li:D ratio was observed in PISCES-B for a 0.1g molten sample at 250-400 °C [72]. Both thick (~500 μm) and thin (<1 μm) Li coatings were exposed to Ne and D plasma in Magnum-PSI [73][74] to study erosion behaviour. This allowed observation of behaviour under high flux (>10^{24} m^{-2} s^{-1}) and to high temperatures (up to 850
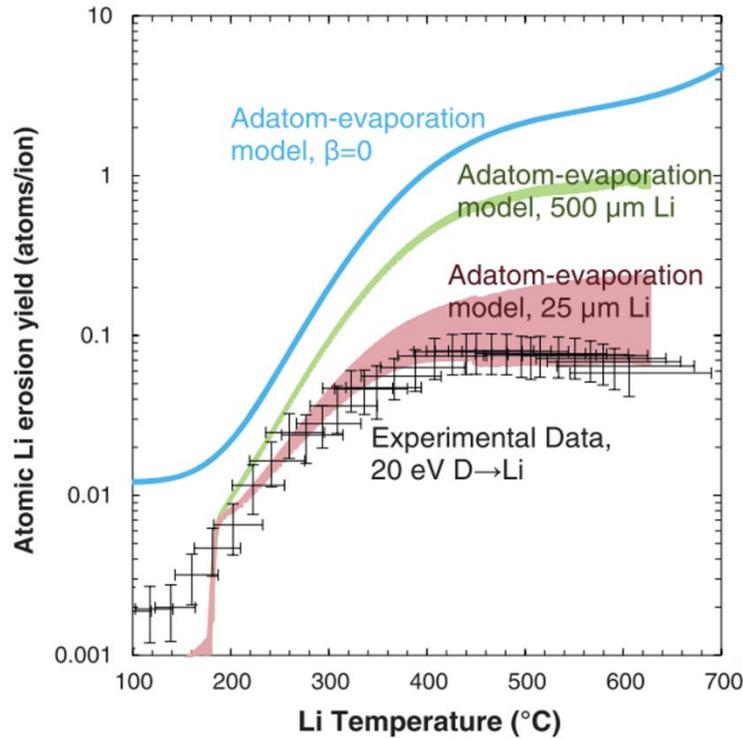
Figure 2: Measured and calculated expected erosion yields for the case of pure Li (β=0) and incorporating the effect of the transformation of pure Li to LiD during the exposure, either with the original layer thickness of 500 μm or with the adjusted thickness of 25 μm due to melt motion. Reproduced from [78].

°C), in comparison to other work [75] [76] lower flux ($<10^{22}$ m^{-2} s^{-1}) and temperatures (<500 °C). For Ne exposures a similar behaviour of anomalous erosion at temperatures below evaporation were observed spectroscopically, but for D the behaviour was significantly different, with erosion rates well below expectations even in the temperature range where Langmuir law [77] evaporation would be expected to be completely dominant. This is attributed firstly to a thinning of the thick Li coatings during the melting process, and secondly to the reduced erosion rate due the interaction of Li and D [78]. Modelling using TRIM.SP [79] indicates that sputtering can be reduced by a factor of 10-40 for a 50:50 Li:D composition in comparison to pure Li, while evaporation can also be strongly reduced due to the higher surface binding energy of LiD (2.26 eV) compared to Li (1.67 eV). The thinner lithium layers are more quickly converted fully to LiD. Combining these two processes can well model the observed results (Figure 2). As a result it can be expected that the upper operational temperature limit for Li dilution may be expected to increase significantly. It should be noted however that a 1:1 Li:D ratio at high temperatures is in disagreement with expectations from studies of molecular hydrogen interaction where only low concentrations are expected at divertor pressures [45], [46] so further study should be carried out to understand the behaviour differences between molecular and radical and ionic hydrogen isotope interaction. Furthermore for a flowing liquid surface it is uncertain whether such a fully saturated surface would be achieved. For now this effect, though likely beneficial in the sense of increasing the temperature range, is also neglected in modelling of power handling limits.

One other area in which operational temperature window limits could be increased is through strong redeposition. At the divertor strikepoints in DEMO and ITER the electron density will be very high and the plasma will enter the strongly-coupled regime where collisional path lengths are short in comparison to the scale lengths of the plasma [80]. In this case a large fraction of recycled and eroded particles are expected to locally ionize and redeposit. Such plasma conditions are achieved in Pilot-PSI and Magnum-PSI, making them good test-beds in studying this process. One difficulty however is in determining in absolute terms the erosion

rate in the plasma. In typically used spectroscopic methods a knowledge of plasma species temperature, electron densities and atomic process rate coefficients is typically needed, and for Sn such coefficients are not available in databases such as ADAS [81]. Therefore a cavity ring-down spectroscopy system was installed at Pilot-PSI to study this directly [82]. This laser absorption technique gives an absolute plasma species population measurement by determining the decay time of a laser pulse trapped in a high-finesse optical cavity which the plasma passes through close to the target position. Biased Sn CPS targets were exposed to Ar plasma at fluxes 1.6-2.7×10^{23} m^{-2} s^{-1} and temperatures up to 1150 °C, just below where evaporation should start to dominate erosion under those conditions. In comparing the observed amount of eroded particles to that expected from sputtering and evaporation around three orders of magnitude fewer Sn^0 atoms were observed than would be expected from the model, even after accounting for experimental uncertainties and geometric losses. This can be accounted for by a combination of ion-neutral friction and ionization which leads to plasma entrainment in the flow towards the target surface and redeposition at the target. This implies a redeposition rate of 98-99.8% which
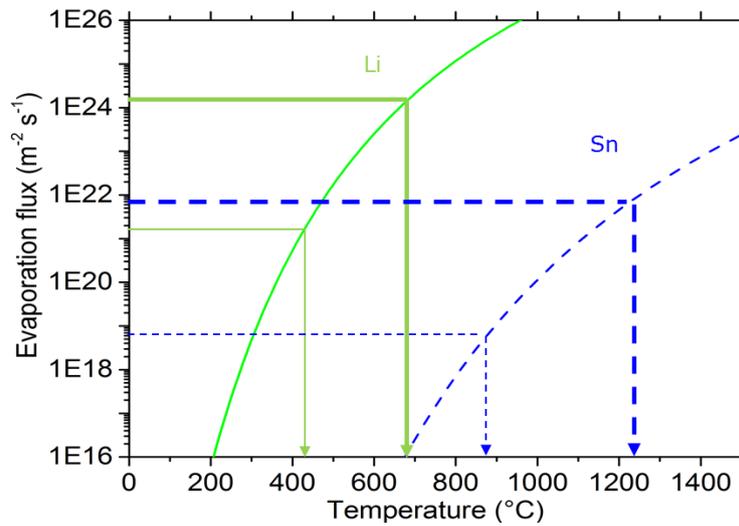

Figure 3: Evaporation rates of Li (solid) and Sn (dashed) showing the temperature limits determined from equation 1 with either a redeposition rate of zero (thin lines) or of 99.9% (thick lines).

would increase the operational temperature window to around 1250 °C in the regime where evaporation is dominant [25] (Figure 3). A similar behaviour would be expected for Li and would give an increase to around 700 °C. For Sn this increase is useful but not definitive but a similar effect could be of higher importance for the use of Li where the temperature window is otherwise much smaller given the requirement to operate at relatively high temperatures to avoid excessive T retention.

2.3 Power handling and vapour shielding

Ultimately one of the main questions for the use of liquid metals in a PFC is whether such a component is able to sustain a similar or greater heat-load than the baseline DEMO designs. To determine this requires an accurate understanding of the thermal properties of a CPS material, which is a mixture of at least two different component elements. Using a series of high heat flux He discharges in Pilot-PSI on a Sn-W CPS (40:60 volume ratio) it was demonstrated via comparison with finite element modelling that the thermal conductivity of the CPS could best be described using the rule of mixtures, i.e. $k_{CPS} = \sum_i V_i k_i$ where V_i and k_i are the volume fraction and thermal conductivity of element i [26]. Using this description it was possible to use
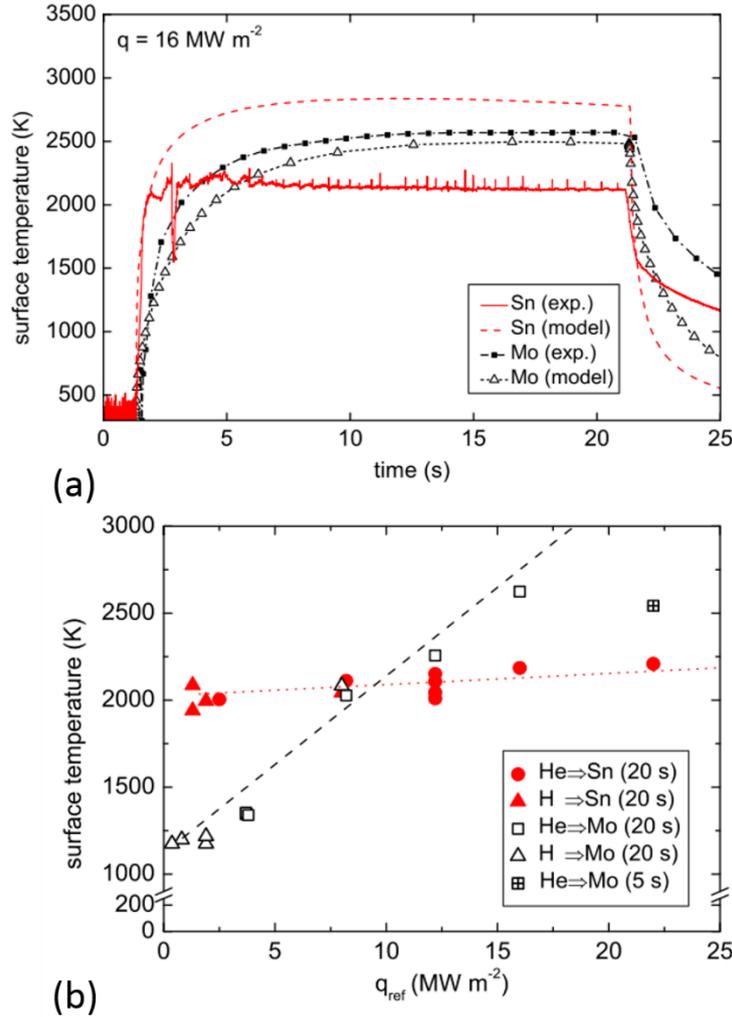
Figure 4:(a) Temperature evolution of the Sn and Mo samples, showing the locking behaviour in the case of Sn. The modelled predictions using ANSYS are also shown assuming conduction cooling only. (b) maximum surface temperature reached at the end of the discharge where temperature equilibrium is reached in all cases, excepting the 5 second shot. Unlike for the expected behaviour of the Mo sample the Sn sample approaches a similar surface temperature in all cases. Reproduced from [97]

finite element modelling to modify existing models of DEMO divertor PFCs [83] by adding a thin CPS layer to the surface. The heat load limits were computed via comparing the temperature limits for each part of the component, assigning evaporation limits for Sn as in [25], which is equivalent to a redeposition rate of ~90%. In the direct comparison where the top 1 mm is replaced by a Sn-W CPS layer a slightly lower maximum heat load is achievable: 15 MW m^{-2} compared to 18 MW m^{-2}, but potentially other alterations such as thinning and shrinking the component due to a relaxation in the W-erosion thickness requirement would raise the operating limit to 20 MW m^{-2}. Alternatively using a full CPS layer and replacing the CuCrZr pipe with a EUROFER pipe would still deliver 15 MW m^{-2} while being expected to strongly reduce stress in the component and reduce activation levels. Furthermore eliminating CuCrZr would be beneficial due to its inferior performance under neutron loading compared to EUROFER [84]. Clearly such designs, while based on detailed analysis for W-based components, require a much more complete evaluation. However they appear promising, and form a starting point for developing a full conceptual design for DEMO.

The work previously described relied only on conduction based cooling. Unlike solid targets however, strong evaporation at elevated temperatures is intrinsically present for liquid targets. The interaction of the vapour with the plasma can absorb part of the incoming power, reducing
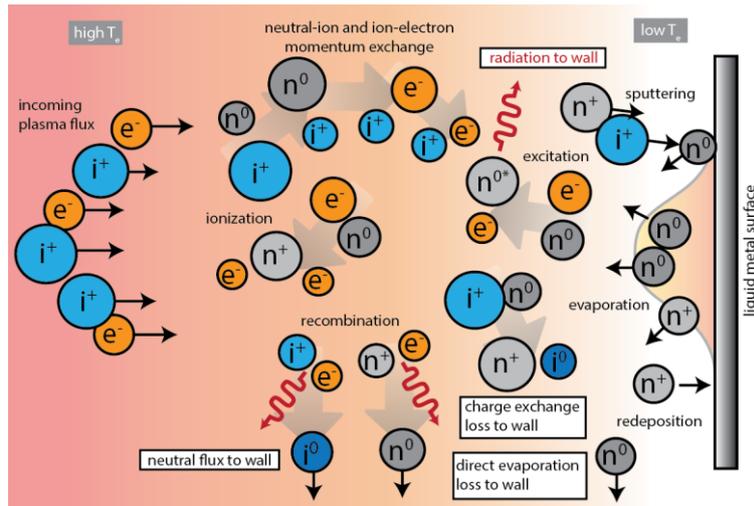
8

Figure 5: A schematic illustration of the major atomic processes taking place during vapour shielding and the loss channels which remove part of the heat before it reaches the LM surface.

loading to the substrate. Such an effect has been predicted and modelled for disruptions [27] and studied in plasma guns [85] but for liquid metals had not previously been experimentally demonstrated. This was done using Sn-W CPS targets exposed to H and He plasmas to heat fluxes of 0.5-22 MW m^{-2} with deliberately poorly cooled targets [86]. Strikingly the surface temperature during the plasma discharge rises to a nearly fixed temperature (~1700-1900 °C), which is nearly constant across a very wide range of heat fluxes (Figure 4). This decoupling contrasts to the response of a Mo reference where the equilibrium temperature is proportional to the heat flux as would be expected from Fourier's law. This behaviour can be explained through a combination of direct evaporation removing heat from the surface (up to 20%), direct radiation and ion-neutral friction. The combined effect was found to lead to electron temperatures <0.5 eV compared to 2-3 eV for the reference target, leading to an enhancement in recombination. This, in combination with charge exchange can lead to a mass and energy loss channel which further removes power from the plasma before it reaches the surface (Figure 5). Overall a reduction of around one third in the power to the surface was found via cooling water calorimetry. As evaporation is a strong function of surface temperature it was postulated to act as a negative feedback system. It was found that the temperature locking takes place when the evaporative flux is approximately 1.6× that of the incoming particle flux over the range Γ=1-6.5×10^{24} m^{-2} s^{-1}. At this balance point the energy losses due to the plasma interaction with the vapour are enough to reduce the heat load interacting with the surface to match the conduction cooling rate, preventing any additional temperature rise. Likewise any reduction in evaporation would lead to an increase in incoming heat loading which would raise the temperature and thus evaporation rate. It seems clear that a high density environment in the divertor is also required in this case such that many collisions and atomic processes take place locally and remove power from the strikepoint region. This type of regime is expected in DEMO.

A more detailed examination of the phenomenon identified it as an oscillatory phenomenon [87] due to the difference in heating and cooling rates at the edge and centre of the plasma beam and the fast atomic and molecular processes in comparison with the slower cooling time and even slower heating time. At the beam centre the equilibrium point is reached rapidly while this
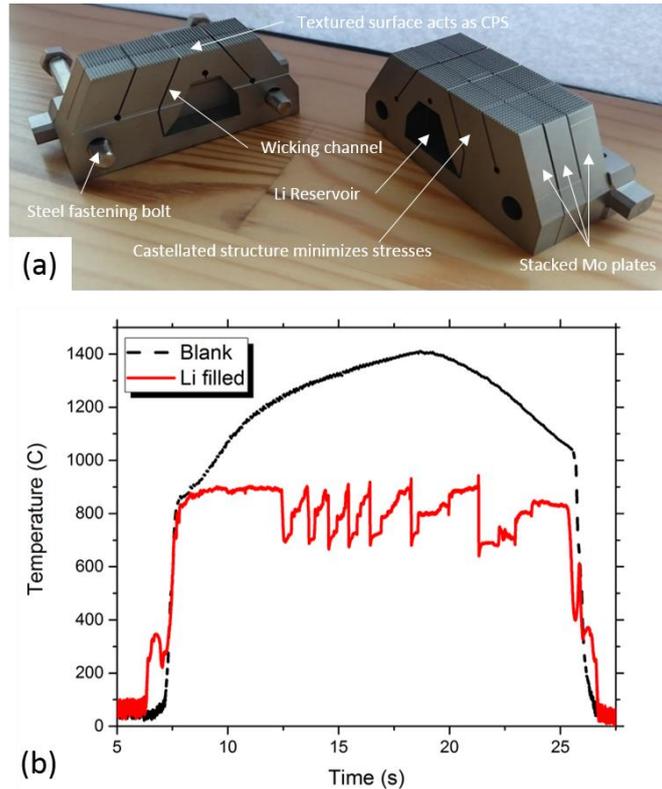
Figure 6: (a) photo of the target used for Li vapour shielding experiments prior to Li filling and closure. The sample was constructed from Mo plates held together with bolts. A textured surface to act as a CPS system and wicking channels were cut using EDM. (b) Temperature response of the Li filled sample at the beam spot centre compared to the temperature response of an identical unfilled (blank) sample, showing the temperature locking behaviour.

occurs more slowly at the edge due to the lower heat load. Once the edge regions also approach the central temperature a critical particle density appears to be reached and a full detachment-like state occurs where the entire surface rapidly cools while temporarily the vapour cloud remains extended. This is linked to reaching a low electron temperature where recombination leads to further temperature reduction in a positive feedback. Following this the surface cools relatively uniformly until the evaporative flux is lower. A period of heating occurs where the plasma is temporarily reattached and electron temperatures are measured to briefly recover, and the cycle repeats. The timescale is set by the difference in cooling rates and heating rates which are much slower due to the near balance between incoming and removed heat loads. This phenomenon seems general for any high density and heat flux plasma as would be expected at the strikepoints and might therefore be expected in DEMO also.

For Sn the vapour shielding effect occurs at temperatures which are beyond the long term material compatibility limits of potential substrates [88][89] and thus may not be generally applicable except in the case of off-normal loading where it could act as a self-protection mechanism. For Li however the vapour pressure is higher, and it was predicted [87] that a similar behaviour should be expected for surface temperatures around 700 °C. This was investigated using samples designed with a pre-filled reservoir of Li to resupply lost Li to the plasma facing surface. The details of the recent experiments will be described in a forthcoming publication, but a photo of the sample design is shown in Figure 6(a). A temperature trace of the He plasma exposure of a filled target and an empty one with no Li present are shown in Figure 6(b). A similar temperature locking behaviour is observed which indicates that the vapour shielding effect is also present. The temperature locking also occurs at a temperature of ~700-900 °C, in agreement with the predictions of [87].
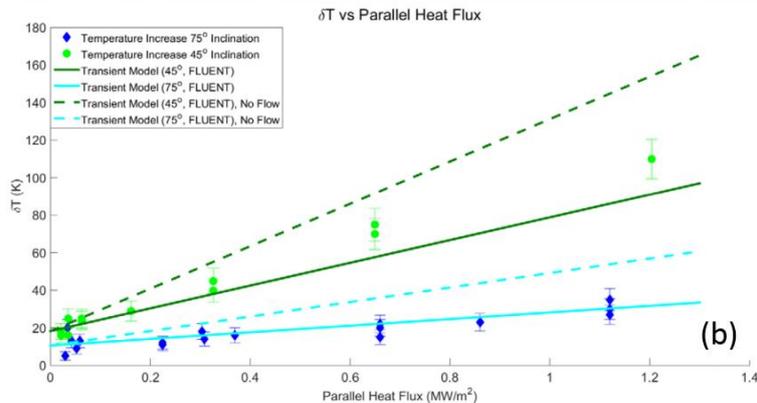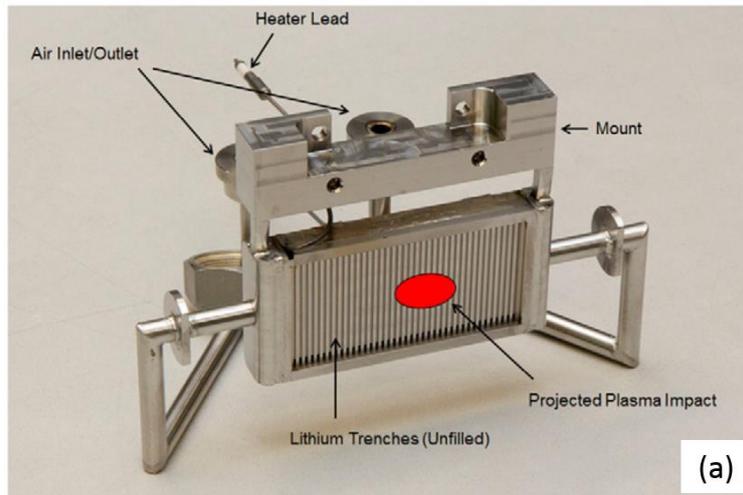
Figure 7: (a) Photograph of the LiMIT test module with important parts labelled prior to exposure in Magnum-PSI. The module is constructed of stainless steel with air cooling channels in the centre. A heater at the backside ensures the module stayed above the Li melting temperature. (b) the temperature response of the lithium at the centre of the plasma beam for two different inclination angles under different parallel heat loads (points). The dashed lines indicate the modelled response for the case of conduction only while the solid lines are the modelled predicted temperature response where convection is also included. Figures taken from [98].

All previous work relied upon the CPS system for capillary restraint of the liquid. This removed any capacity for convective cooling. One more complex design which incorporates liquid flow is the Liquid Metal Infused Trench (LiMIT) concept [30]. This concept uses thin trenches to confine the liquid metal using surface tension, while driving flow along the trenches using the thermoelectric magnetohydrodynamic force [90], [91] that arises due to the combination of a thermoelectric current due to the thermal gradient between top and bottom of the trench and the magnetic field component orthogonal to the thermal gradient and trench direction. This produces a flow driven by and proportional to the plasma heat flux which can convect part of the heat load away from the strikepoint area. This concept had previously been tested in the laboratory using electron beam loading [30], [92] and in the tokamak HT-7 [93], and a test module was constructed and tested in Magnum-PSI under high heat and plasma flux loading (Figure 7a). The channels of the module were filled in-situ with a Li injection needle [94] and could flow along the trenches which surrounded the cooling channels on all sides. Amongst other things, the temperature response at the plasma beam centre was monitored and compared to a 3D time-dependent heat transfer simulation of the trench using FLUENT [95]. This clearly demonstrated that the induced flow lead to a significant reduction in the peak temperature due

11

to the contribution of convection in redistributing the heat to other parts of the module (Figure 7b). If such a flowing system could be incorporated into a LM PFC it could aid in minimizing the peak surface temperature at the divertor strikepoints, which could be significant in optimizing performance and the maximum heat load, which is likely to be most strongly linked to evaporation limits.

3. Conclusion

The use of linear devices Magnum-PSI and Pilot-PSI have been shown to give significant insight into determining the future performance of liquid metals as a PFM for a future fusion power plant. In defining an operational range for these materials in terms of maximum power density it seems clear that this is likely to be defined by the maximum tolerable impurity content and thus indirectly by the net erosion rate and thus temperature range in the case that evaporation is dominant. We should assess separately at this point the case for Sn and for Li.

For a Sn based CPS-type design 20 MW m^{-2} seems feasible employing only conduction with a thin CPS layer on top of a thin W water cooled component [26]. It should be noted that in that case the upper power handling limit was due to the temperature limit of the CuCrZr pipe compared rather than the temperature limit for evaporation (taken as 1000 °C, i.e. assuming a 90% redeposition rate for Sn). It may be feasible to design components where Sn evaporation is the limiting factor, especially given there are very large uncertainties in the tolerable erosion flux. In this case a high redeposition rate as measured in [82] and as would be expected in the highly dense partially detached divertor conditions in DEMO would be able to increase the operational temperature range and the power handling by as much as an additional 5 MW m^{-2} [26]. Erosion by stannane production may be of concern as an additional source of Sn and little is known about its behaviour under fusion-relevant conditions. Currently it is assumed not to be the critical limit for power handling as evaporation is expected to dominate. Vapour shielding would not be expected to play a significant role for a Sn based component under normal operating conditions due to the high required temperature. However in the case of off-normal heat loading such temperatures could be reached and dissipate significant power, protecting the underlying substrate from permanent damage. In particular this would be beneficial in permitting some ELMs and in enabling resumption of operation without maintenance after a disruption for example [96].

For Li the evaporation pressure is much higher than Sn, and therefore despite their similar melting points the limit where the evaporation rate is too high is reached at much lower temperatures. Extrapolating from [26] and assuming a similar k_{CPS} for the combination W and Li as for W and Sn gives an approximate power handling capability of around 7.5 MW m^{-2}. However, this neglects the strong interaction between Li and D which reduces the erosion rate and thus in combination with a high redeposition rate could increase the maximum tolerable surface temperature to above 700 °C assuming the limits given in section 2.2. This brings the power handling limit to around 12.5 MW m^{-2} optimistically. This also raises the temperature limit to that expected for vapour shielding to be effective based on the initial results presented here. In such a case the temperature locking effect would be expected to hold the temperature at this point as the power is increased, avoiding excessive dilution of the core plasma by evaporation. Finally if a convective system could be further developed for either Li or Sn, for example employing the principles explored using the LiMIT system in section 2.3, higher power loading could be tolerated by additionally removing heat from the strikepoint region, but it should be noted that is far from practical realization.

Overall the results are promising for the development of a liquid metal CPS. However, many questions remain that should be addressed. Generally the concept requires a much firmer engineering basis, incorporating the entire LM cycle of replenishment, the detailed plasma

facing unit design including cooling and compatibility of substrate materials, as well as the influence of metal vapour on vacuum systems. Generally more work is needed on performance under transient loading, which is not addressed here, particularly the vapour shielding and surface replenishment rate. For Li ensuring temperatures everywhere are above the temperature limit for gas phase absorption of T would be a strong challenge, as well as how to cool the substrate if safety restrictions would prevent water cooling for Li due to its strong reactivity. For Sn more studies should be made as to the production and decomposition of stannane under fusion reactor conditions. For both modelling and tokamak experiments should identify in more detail the baffling, pumping and erosion requirements in limiting core impurity accumulation to manageable levels.

Despite this list of areas where more research is required, it should be noted that significant progress has been made through the use of liquid metals for future PFCs. In conclusion it seems promising that liquid-metal based PFCs can extend the lifetime of the divertor and can potentially greatly increase the availability and economic viability of a fusion reactor.

4. Acknowledgements

5. Bibliography

[1]   "ITER Physics Basis," *Nucl. Fusion*, vol. 39, no. 12, p. 2137, 1999.

[2]   K. Ikeda, "Progress in the ITER Physics Basis," *Nucl. Fusion*, vol. 47, no. 6, 2007.

[3]   G. Federici, C. Bachmann, W. Biel, L. Boccaccini, F. Cismondi, S. Ciattaglia, M. Coleman, C. Day, E. Diegele, T. Franke, M. Grattarola, H. Hurzlmeier, A. Ibarra, A. Loving, F. Maviglia, B. Meszaros, C. Morlock, M. Rieth, M. Shannon, N. Taylor, M. Q. Tran, J. H. You, R. Wenninger, and L. Zani, "Overview of the design approach and prioritization of R&D activities towards an EU DEMO," *Fusion Eng. Des.*, vol. 109–111, pp. 1464–1474, 2016.

[4]   F. Romanelli, "Fusion Electricity A roadmap to the realisation of fusion energy (https://www.euro-fusion.org/wpcms/wp-content/uploads/2013/01/JG12.356-web.pdf (accessed 19-06-2017)," 2013.

[5]   M. R. Gilbert, S. Zheng, R. Kemp, L. W. Packer, and S. L. Dudarev, "COMPARATIVE ASSESSMENT OF MATERIAL PERFORMANCE IN DEMO FUSION REACTORS," *Fusion Sci. Technol.*, vol. 66, no. 2013, pp. 9–17, 2014.

[6]   G. Federici, R. Kemp, D. Ward, C. Bachmann, T. Franke, S. Gonzalez, C. Lowry, M. Gadomska, J. Harman, B. Meszaros, C. Morlock, F. Romanelli, and R. Wenninger, "Overview of EU DEMO design and R&D activities," *Fusion Eng. Des.*, vol. 89, no. 7–8, pp. 882–889, 2014.

[7]   A. Kallenbach, M. Bernert, R. Dux, L. Casali, T. Eich, L. Giannone, A. Herrmann, R. McDermott, A. Mlynek, H. W. Müller, F. Reimold, J. Schweinzer, M. Sertoli, G. Tardini,

W. Treutterer, E. Viezzer, R. Wenninger, and M. Wischmeier, "Impurity seeding for tokamak power exhaust: from present devices via ITER to DEMO," *Plasma Phys. Control. Fusion*, vol. 55, no. 12, p. 124041, Dec. 2013.

[8] Y. R. Martin, T. Takizuka, and ITPA CDBM H-mode Threshold Database Working Group, "Power requirement for accessing the H-mode in ITER," *J. Phys. Conf. Ser.*, vol. 123, p. 12033, 2008.

[9] H. Zohm, C. Angioni, E. Fable, G. Federici, G. Gantenbein, T. Hartmann, K. Lackner, E. Poli, L. Porte, O. Sauter, G. Tardini, D. Ward, and M. Wischmeier, "On the physics guidelines for a tokamak DEMO," *Nucl. Fusion*, vol. 53, no. 7, p. 73019, Jul. 2013.

[10] M. R. Gilbert and J.-C. Sublet, "Neutron-induced transmutation effects in W and W-alloys in a fusion environment," *Nucl. Fusion*, vol. 51, p. 43005, 2011.

[11] G. Pintsuk, *Tungsten as a Plasma-Facing Material*. Amsterdam: Elsevier Inc., 2012.

[12] D. Maisonnier, D. Campbell, I. Cook, L. Di Pace, L. Giancarli, J. Hayward, a. Li Puma, M. Medrano, P. Norajitra, M. Roccella, P. Sardain, M. Q. Tran, and D. Ward, "Power plant conceptual studies in Europe," *Nucl. Fusion*, vol. 47, no. 11, pp. 1524–1532, Nov. 2007.

[13] J. Linke, T. Loewenhoff, V. Massaut, G. Pintsuk, G. Ritz, M. Rödig, a. Schmidt, C. Thomser, I. Uytdenhouwen, V. Vasechko, and M. Wirtz, "Performance of different tungsten grades under transient thermal loads," *Nucl. Fusion*, vol. 51, no. 7, p. 73017, Jul. 2011.

[14] T. Hirai, S. Panayotis, V. Barabash, C. Amzallag, F. Escourbiac, A. Durocher, M. Merola, J. Linke, T. Loewenhoff, G. Pintsuk, M. Wirtz, and I. Uytdenhouwen, "Use of tungsten material for the ITER divertor," *Nucl. Mater. Energy*, vol. 9, no. 2016, pp. 616–622, 2016.

[15] G. G. van Eden, T. W. Morgan, H. J. van der Meiden, J. Matejicek, T. Chraska, M. Wirtz, and G. De Temmerman, "The effect of high-flux H plasma exposure with simultaneous transient heat loads on tungsten surface damage and power handling," *Nucl. Fusion*, vol. 54, no. 12, p. 123010, 2014.

[16] M. Wirtz, S. Bardin, A. Huber, A. Kreter, J. Linke, T. W. Morgan, G. Pintsuk, M. Reinhart, G. Sergienko, I. Steudel, G. De Temmerman, and B. Unterberg, "Impact of combined hydrogen plasma and transient heat loads on the performance of tungsten as plasma facing material," *Nucl. Fusion*, vol. 55, no. 12, 2015.

[17] S. Bardin, T. W. Morgan, R. A. Pitts, and G. De Temmerman, "Evolution of transient melt damaged tungsten under ITER-relevant divertor plasma heat loading," *J. Nucl. Mater.*, vol. 463, p. 1400, 2015.

[18] T. Loewenhoff, a Bürger, J. Linke, G. Pintsuk, a Schmidt, L. Singheiser, and C. Thomser, "Evolution of tungsten degradation under combined high cycle edge-localized mode and steady-state heat loads," *Phys. Scr.*, vol. T145, p. 14057, 2011.

[19] T. Loewenhoff, J. Linke, G. Pintsuk, and C. Thomser, "Tungsten and CFC degradation under combined high cycle transient and steady state heat loads," *Fusion Eng. Des.*, vol. 87, no. 7–8, pp. 1201–1205, Aug. 2012.

[20] R. A. Pitts, S. Carpentier, F. Escourbiac, T. Hirai, V. Komarov, S. Lisgo, A. S. Kukushkin, A. Loarte, M. Merola, A. Sashala Naik, R. Mitteau, M. Sugihara, B. Bazylev, and P. C. Stangeby, "A full tungsten divertor for ITER: Physics issues and design status," *J. Nucl. Mater.*, vol. 438, pp. S48–S56, Jul. 2013.

[21] J. P. Gunn, S. Carpentier-Chouchana, F. Escourbiac, T. Hirai, S. Panayoutis, R. A. Pitts, Y. Corre, R. Dejarnac, M. Firdaouss, M. Kocan, M. Komm, A. S. Kukushkin, P.

Languille, M. Missirlian, W. Zhao, and G. Zhong, "Surface heat loads on the ITER divertor vertical targets," *Nucl. Fusion*, vol. 57, 2017.

[22] H. Iida, V. Khripunov, and L. Petrizzi, "ITER Report G 73 DDD 2 W 0.2 (Nuclear Analysis Report)," p. 229, 2001.

[23] F. Hofmann, D. R. Mason, J. K. Eliason, A. A. Maznev, K. A. Nelson, and S. L. Dudarev, "Non-Contact Measurement of Thermal Diffusivity in Ion-Implanted Nuclear Materials," *Sci. Rep.*, vol. 5, p. 16042, 2015.

[24] V. Barabash, G. Federici, M. Rödig, L. L. Snead, and C. H. Wu, "Neutron irradiation effects on plasma facing materials," *Journal of Nuclear Materials*, vol. 283–287, no. PART I. pp. 138–146, 2000.

[25] J. W. Coenen, G. De Temmerman, G. Federici, V. Philipps, G. Sergienko, G. Strohmayer, a Terra, B. Unterberg, T. Wegener, and D. C. M. Van den Bekerom, "Liquid metals as alternative solution for the power exhaust of future fusion devices: status and perspective," *Phys. Scr.*, vol. T159, p. 14037, Apr. 2014.

[26] T. W. Morgan, A. Vertkov, K. Bystrov, I. Lyublinski, and J. W. Genuit, "Power handling of a liquid-metal based CPS structure under high steady-state heat and particle fluxes," *Nucl. Mater. Energy*, vol. 0, pp. 1–6, 2017.

[27] A. Hassanein, T. Sizyuk, and I. Konkashbaev, "Integrated simulation of plasma surface interaction during edge localized modes and disruptions: Self-consistent approach," *J. Nucl. Mater.*, vol. 390–391, pp. 777–780, Jun. 2009.

[28] Y. Nagayama, "Liquid lithium divertor system for fusion reactor," *Fusion Eng. Des.*, vol. 84, no. 7–11, pp. 1380–1383, Jun. 2009.

[29] R. J. Goldston, R. Myers, and J. Schwartz, "The lithium vapor box divertor," *Phys. Scr.*, vol. T167, p. 14017, 2016.

[30] D. N. Ruzic, W. Xu, D. Andruczyk, and M. a. Jaworski, "Lithium–metal infused trenches (LiMIT) for heat removal in fusion devices," *Nucl. Fusion*, vol. 51, no. 10, p. 102002, Oct. 2011.

[31] M. Shimada and Y. Hirooka, "Actively convected liquid metal divertor," *Nucl. Fusion*, vol. 54, no. 12, p. 122002, Dec. 2014.

[32] M. Ono, M. a. Jaworski, R. Kaita, Y. Hirooka, D. Andruczyk, and T. K. Gray, "Active radiative liquid lithium divertor concept," *Fusion Eng. Des.*, vol. 89, no. 12, pp. 2838–2844, Dec. 2014.

[33] G. De Temmerman, M. a. van den Berg, J. Scholten, a. Lof, H. J. van der Meiden, H. J. N. van Eck, T. W. Morgan, T. M. de Kruijf, P. a. Zeijlmans van Emmichoven, and J. J. Zielinski, "High heat flux capabilities of the Magnum-PSI linear plasma device," *Fusion Eng. Des.*, vol. 88, no. 6–8, pp. 483–487, Oct. 2013.

[34] H. J. N. Van Eck, T. Abrams, M. A. Van Den Berg, S. Brons, G. G. Van Eden, M. A. Jaworski, R. Kaita, H. J. Van Der Meiden, T. W. Morgan, M. J. Van De Pol, J. Scholten, P. H. M. Smeets, G. De Temmerman, P. C. De Vries, and P. A. Zeijlmans Van Emmichoven, "Operational characteristics of the high flux plasma generator Magnum-PSI," *Fusion Eng. Des.*, vol. 89, no. 9–10, 2014.

[35] G. J. van Rooij, V. P. Veremiyenko, W. J. Goedheer, B. de Groot, A. W. Kleyn, P. Smeets, and T. W. Versloot, "Extreme hydrogen plasma densities achieved in a linear plasma generator," *Appl. Phys. Lett.*, vol. 90, p. 121501, 2007.

[36] G. De Temmerman, J. J. Zielinski, S. van Diepen, L. Marot, and M. Price, "ELM simulation experiments on Pilot-PSI using simultaneous high flux plasma and transient heat/particle source," *Nucl. Fusion*, vol. 51, no. 7, p. 73008, Jul. 2011.

[37] M. A. Abdou, T. A. Team, A. Ying, N. Morley, K. Gulec, S. Smolentsev, M. Kotschenreuther, S. Malang, S. Zinkle, T. Rognlien, P. Fogarty, B. Nelson, R. Nygren, K. McCarthy, M. Z. Youssef, N. Ghoniem, D. Sze, C. Wong, M. Sawan, H. Khater, R. Woolley, R. Mattas, R. Moir, S. Sharafat, J. Brooks, A. Hassanein, D. Petti, M. Tillack, M. Ulrickson, and T. Uchimoto, "On the exploration of innovative concepts for fusion chamber technology," *Fusion Eng. Des.*, vol. 54, no. 2, pp. 181–247, 2001.

[38] G. Kieselmann, "Ga based alloys and compounds," in *Landolt-Börnstein - Group III Condensed Matter 21A (Ac - Na)*, W. K. R. Flükiger, Ed. Berlin Heidelberg: Springer-Verlag, 1990.

[39] R. A. Forrest, A. Tabasso, C. Danani, S. Jakhar, and A. K. Shaw, "Handbook of Activation Data Calculated Using EASY-2007," 2009.

[40] D. K. Mansfield, K. W. Hill, J. D. Strachan, M. G. Bell, S. D. Scott, R. Budny, E. S. Marmar, J. a. Snipes, J. L. Terry, S. Batha, R. E. Bell, M. Bitter, C. E. Bush, Z. Chang, D. S. Darrow, D. Ernst, E. Fredrickson, B. Grek, H. W. Herrmann, a. Janos, D. L. Jassby, F. C. Jobes, D. W. Johnson, L. C. Johnson, F. M. Levinton, D. R. Mikkelsen, D. Mueller, D. K. Owens, H. Park, a. T. Ramsey, a. L. Roquemore, C. H. Skinner, T. Stevenson, B. C. Stratton, E. Synakowski, G. Taylor, a. von Halle, S. von Goeler, K. L. Wong, and S. J. Zweben, "Enhancement of Tokamak Fusion Test Reactor performance by lithium conditioning," *Phys. Plasmas*, vol. 3, no. 5, p. 1892, 1996.

[41] R. Majeski, M. Boaz, D. Hoffman, B. Jones, R. Kaita, H. Kugel, T. Munsat, J. Spaleta, V. Soukhanovskii, J. Timberlake, L. Zakharov, G. Antar, R. Doerner, S. Luckhardt, R. W. Conn, M. Finkenthal, D. Stutman, R. Maingi, and M. Ulrickson, "Plasma performance improvements with liquid lithium limiters in CDX-U," *Fusion Eng. Des.*, vol. 65, no. 3, pp. 443–447, Apr. 2003.

[42] G. Mazzitelli, M. L. Apicella, D. Frigione, G. Maddaluno, M. Marinucci, C. Mazzotta, V. Pericoli Ridolfini, M. Romanelli, G. Szepesi, and O. Tudisco, "FTU results with a liquid lithium limiter," *Nucl. Fusion*, vol. 51, no. 7, p. 73006, Jul. 2011.

[43] J. S. Hu, G. Z. Zuo, J. Ren, Q. X. Yang, Z. X. Chen, H. Xu, L. E. Zakharov, R. Maingi, C. Gentile, X. C. Meng, Z. Sun, W. Xu, Y. Chen, D. Fan, N. Yan, Y. M. Duan, Z. D. Yang, H. L. Zhao, Y. T. Song, X. D. Zhang, B. N. Wan, and J. G. Li, "First results of the use of a continuously flowing lithium limiter in high performance discharges in the EAST device," *Nucl. Fusion*, vol. 56, no. 4, p. 46011, 2016.

[44] M. A. Abdou, N. B. Morley, S. Smolentsev, A. Ying, S. Malang, A. Rowcliffe, and M. Ulrickson, "Blanket/first wall challenges and required R&D on the pathway to DEMO," *Fusion Eng. Des.*, vol. 100, pp. 2–43, 2015.

[45] E. Veleckis, E. H. Van Deventer, and M. Blander, "The Lithitmi-Lithium Hydride System," *Chem. Eng. Div. Argonne Natl. Lab.*, vol. 60439, no. 19, 1974.

[46] F. J. Smith, J. F. Land, G. M. Begun, and A. M. Gamma de Batiston, "EQUILIBRIUM FOR HYDROGEN ISOTOPES IN LITHIUM," vol. 41, no. 7, pp. 1001–1009, 1979.

[47] C. B. Alcock, V. P. Itkin, and M. K. Horrigan, "Vapor pressure of the metallic elements," *Can. Metall. Quarterly1*, vol. 23, p. 309, 1984.

[48] J. P. S. Loureiro, H. Fernandes, F. L. Tabarés, G. Mazzitelli, C. Silva, R. Gomes, E. Alves, R. Mateus, T. Pereira, H. Figueiredo, and H. Alves, "Deuterium retention in tin (Sn) and lithium-tin (Li-Sn) samples exposed to ISTTOK plasmas," *Nucl. Mater. Energy*, 2016.

[49] S. Sharafat and N. Ghoniem, "Summary of Thermo-Physical Properties of Sn , Comparison of Properties of Sn , Sn-Li , Li , and Pb-Li," *UCLA-UCMEP-00-31 Rep.*, pp. 1–51, 2000.

[50] R. Bastasz and J. a. Whaley, "Surface composition of liquid metals and alloys," *Fusion Eng. Des.*, vol. 72, no. 1–3, pp. 111–119, Nov. 2004.

[51] G. Miloshevsky and A. Hassanein, "Modelling of Kelvin–Helmholtz instability and splashing of melt layers from plasma-facing compoents in tokamaks under plasma impact," *Nucl. Fusion*, vol. 50, p. 115005, 2010.

[52] G. Miloshevsky and a. Hassanein, "Effects of plasma flow velocity on melt-layer splashing and erosion during plasma instabilities," *Nucl. Fusion*, vol. 54, no. 3, p. 33008, 2014.

[53] M. a. Jaworski, T. Abrams, J. P. Allain, M. G. Bell, R. E. Bell, a. Diallo, T. K. Gray, S. P. Gerhardt, R. Kaita, H. W. Kugel, B. P. LeBlanc, R. Maingi, a. G. McLean, J. Menard, R. Nygren, M. Ono, M. Podesta, a. L. Roquemore, S. a. Sabbagh, F. Scotti, C. H. Skinner, V. a. Soukhanovskii, and D. P. Stotler, "Liquid lithium divertor characteristics and plasma–material interactions in NSTX high-performance plasmas," *Nucl. Fusion*, vol. 53, no. 8, p. 83032, Aug. 2013.

[54] D. G. Whyte, T. E. Evans, C. P. C. Wong, W. P. West, R. Bastasz, J. P. Allain, and J. N. Brooks, "Experimental observations of lithium as a plasma-facing surface in the DIII-D tokamak divertor," *Fusion Eng. Des.*, vol. 72, no. 1–3, pp. 133–147, Nov. 2004.

[55] V. A. Evtikhin, I. E. Lyublinski, A. V Vertkov, V. G. Belan, I. K. Konkashbaev, and L. B. Nikandrov, "Calculation and experimental investigation of fusion reactor divertor plate and first wall protection by capillary-pore systems with lithium," *J. Nucl. Mater.*, vol. 272, pp. 396–400, 1999.

[56] P. Fiflis, T. W. Morgan, S. Brons, G. G. Van Eden, M. A. Van Den Berg, W. Xu, D. Curreli, and D. N. Ruzic, "Performance of the lithium metal infused trenches in the magnum PSI linear plasma simulator," *Nucl. Fusion*, vol. 55, no. 11, 2015.

[57] J. L. Cecchi, "Impurity control in TFTR," *J. Nucl. Mater.*, vol. 94, pp. 28–43, 1980.

[58] T. Pütterich, R. Neu, R. Dux, A. D. Whiteford, M. G. O'Mullane, and H. P. Summers, "Calculation and experimental test of the cooling factor of tungsten," *Nucl. Fusion*, vol. 50, no. 2, p. 25012, 2010.

[59] V. Prozesky, "Re-evaluation of tolerable impurity concentrations in a DT fusion plasma based on energy and 4He particle exhaust," *Plasma Phys. Control. Fusion*, vol. 35, pp. 1717–1724, 1993.

[60] J. Roth and W. Möller, "Mechanism of enhanced sputtering of carbon at temperatures above 1200??C," *Nucl. Inst. Methods Phys. Res. B*, vol. 7–8, no. PART 2, pp. 788–792, 1985.

[61] R. P. Doerner, S. I. Krasheninnikov, and K. Schmid, "Particle-induced erosion of materials at elevated temperature," *J. Appl. Phys.*, vol. 95, no. 8, p. 4471, 2004.

[62] G. Federici, C. H. Skinner, J. N. Brooks, J. P. Coad, C. Grisolia, A. A. Haasz, A. Hassanein, V. Phillips, C. S. Pitcher, J. Roth, W. R. Wampler, and D. G. Whyte, "Plasma-material interactions in current tokamaks and their implications for next step fusion reactors," *Nucl. Fusion*, vol. 41, no. 12B, pp. 1967–2137, 2001.

[63] M. D. Coventry, J. P. Allain, and D. N. Ruzic, "D+, He+ and H+ sputtering of solid and liquid phase tin," *J. Nucl. Mater.*, vol. 313–316, pp. 636–640, 2003.

[64] M. D. Coventry, J. P. Allain, and D. N. Ruzic, "Temperature dependence of liquid Sn sputtering by low-energy He+ and D+ bombardment," *J. Nucl. Mater.*, vol. 335, no. 1, pp. 115–120, Oct. 2004.

[65] T. W. Morgan, D. C. M. Van Den Bekerom, and G. De Temmerman, "Interaction of a tin-based capillary porous structure with ITER/DEMO relevant plasma conditions," *J.*

Nucl. Mater., vol. 463, pp. 1256–1259, 2015.

[66] R. P. Doerner, M. J. Baldwin, S. I. Krasheninnikov, and K. Schmid, "High temperature erosion of beryllium," *J. Nucl. Mater.*, vol. 337–339, pp. 877–881, Mar. 2005.

[67] Y. Kudriavtsev, a. Villegas, a. Godines, and R. Asomoza, "Calculation of the surface binding energy for ion sputtered particles," *Appl. Surf. Sci.*, vol. 239, no. 3–4, pp. 273–278, Jan. 2005.

[68] T. Pearson, P. Robinson, and E. Stoddart, "The behaviour of metals, particularly lead and bismuth, in atomic hydrogen, and attempts to prepare atomic hydrogen from hydrides," *Proc. R. Soc. London, Ser. A, , Contain. Pap. a Math. Phys. Character*, vol. 142.846, pp. 275–285, 1933.

[69] W. Grochala and P. P. Edwards, "Thermal decomposition of the non-interstitial hydrides for the storage and production of hydrogen," *Chem. Rev.*, vol. 104, no. 3, pp. 1283–1315, 2004.

[70] B. S. F. A. Kettle, "Kettle. 2569 494. The Kinetics of the Decomposition of Stannane on a Tin Surface.," pp. 1956–1959, 1961.

[71] K. Tamaru, "The Thermal Decomposition of Tin Hydride," *J. Phys. Chem.*, vol. 60, no. 5, pp. 610–612, 1956.

[72] M. J. Baldwin, R. P. Doerner, S. C. Luckhardt, and R. W. Conn, "Deuterium retention in liquid lithium," *Nucl. Fusion*, vol. 42, no. 11, pp. 1318–1323, 2002.

[73] T. Abrams, M. a. Jaworski, R. Kaita, D. P. Stotler, G. De Temmerman, T. W. Morgan, M. a. van den Berg, and H. J. van der Meiden, "Erosion of lithium coatings on TZM molybdenum and graphite during high-flux plasma bombardment," *Fusion Eng. Des.*, vol. 89, no. 12, pp. 2857–2863, Dec. 2014.

[74] T. Abrams, M. A. Jaworski, R. Kaita, J. H. Nichols, D. P. Stotler, G. De Temmerman, M. A. van den Berg, H. J. van der Meiden, and T. W. Morgan, "Modeling the reduction of gross lithium erosion observed under high-flux deuterium bombardment," *J. Nucl. Mater.*, vol. 463, pp. 1169–1172, 2015.

[75] R. P. Doerner, M. J. Baldwin, R. W. Conn, a. a. Grossman, S. C. Luckhardt, R. Seraydarian, G. R. Tynan, and D. G. Whyte, "Measurements of erosion mechanisms from solid and liquid materials in PISCES-B," *J. Nucl. Mater.*, vol. 290–293, pp. 166–172, Mar. 2001.

[76] J. P. Allain, M. D. Coventry, and D. N. Ruzic, "Collisional and thermal effects on liquid lithium sputtering," *Phys. Rev. B - Condens. Matter Mater. Phys.*, vol. 76, no. 20, pp. 1–12, 2007.

[77] I. Langmuir, "The vapor pressure of metallic tungsten," *Phys. Rev.*, vol. II, no. 5, pp. 329–342, 1913.

[78] T. Abrams, M. A. Jaworski, M. Chen, E. A. Carter, R. Kaita, D. P. Stotler, G. De Temmerman, T. W. Morgan, M. A. van den Berg, and H. J. van der Meiden, "Suppressed gross erosion of high-temperature lithium via rapid deuterium implantation," *Nucl. Fusion*, vol. 56, no. 1, p. 16022, 2016.

[79] J. P. Biersack and W. Eckstein, "Sputtering studies with the Monte Carlo Program TRIM.SP," *Appl. Phys. A Solids Surfaces*, vol. 34, no. 2, pp. 73–94, 1984.

[80] A. W. Kleyn, N. J. Lopes Cardozo, and U. Samm, "Plasma-surface interaction in the context of ITER.," *Phys. Chem. Chem. Phys.*, vol. 8, no. 15, pp. 1761–74, Apr. 2006.

[81] H. P. Summers, "The ADAS User Manual, version 2.6 http://adas.ac.uk. (accessed 16-06-2017)," 2004.

[82] V. Kvon, R. S. Al, K. Bystrov, F. Peeters, M. C. M. van de Sanden, and T. W. Morgan,

"Tin re-deposition and erosion measured by Cavity-Ring-Down-Spectroscopy under a high flux plasma beam," *Nucl. Fusion*, vol. accepted f, 2017.

[83] A. Li-Puma, M. Richou, P. Magaud, M. Missirlian, E. Visca, and V. P. Ridolfini, "Potential and limits of water cooled divertor concepts based on monoblock design as possible candidates for a DEMO reactor," *Fusion Eng. Des.*, vol. 88, no. 9–10, pp. 1836–1843, 2013.

[84] J. Reiser and M. Rieth, "Optimization and limitations of known DEMO divertor concepts," *Fusion Eng. Des.*, vol. 87, no. 5–6, pp. 718–721, 2012.

[85] V. I. Tereshin, A. N. Bandura, O. V Byrka, V. V Chebotarev, I. E. Garkusha, I. Landman, V. A. Makhlaj, and D. G. Solyakov, "Simulation of ITER Transient Heat Loads to the Divertor Surfaces with Using the High Power Quasi-Steady-State Plasma Accelerator," in *Proceedings of 22nd IAEA Fusion Energy Conference*, 2008, pp. 2–9.

[86] G. G. van Eden, T. W. Morgan, D. U. B. Aussems, M. A. van den Berg, K. Bystrov, and M. C. M. van de Sanden, "Self-Regulated Plasma Heat Flux Mitigation Due to Liquid Sn Vapor Shielding," *Phys. Rev. Lett.*, vol. 116, no. 13, p. 135002, 2016.

[87] G. G. van Eden, V. Kvon, M. C. M. van de Sanden, and T. W. Morgan, "Oscillatory vapour shielding of liquid metal walls in nuclear fusion devices," *Nat. Commun. (accepted Publ.*, 2017.

[88] T. Wegener, "Investigations of Liquid Metals as a First Wall Material for Fusion Reactors at the Linear Plasma Device PSI-2," Aachen University of Applied Sciences, 2013.

[89] A. Vertkov, I. Lyublinski, M. Zharkov, G. Mazzitelli, M. L. Apicella, and M. Iafrati, "Liquid tin limiter for FTU tokamak," *Fusion Eng. Des.*, vol. 117, pp. 130–134, 2017.

[90] J. A. Shercliff, "Thermoelectric magnetohydrodynamics," *J. Fluid Mech.*, vol. 91, pp. 231–251, 1979.

[91] M. A. Jaworski, T. K. Gray, M. Antonelli, J. J. Kim, C. Y. Lau, M. B. Lee, M. J. Neumann, W. Xu, and D. N. Ruzic, "Thermoelectric magnetohydrodynamic stirring of liquid metals," *Phys. Rev. Lett.*, vol. 104, no. 9, pp. 1–4, 2010.

[92] W. Xu, D. Curreli, D. Andruczyk, T. Mui, R. Switts, and D. N. Ruzic, "Heat transfer of TEMHD driven lithium flow in stainless steel trenches," *J. Nucl. Mater.*, vol. 438, no. 422–425, 2013.

[93] J. Ren, G. Zuo, Z. Sun, J. Li, D. Ruzic, and L. Zakharov, "First results of flowing liquid lithium limiter in HT-7," *Phys. Scr.*, vol. T159, p. 14033, 2014.

[94] P. Fiflis, A. Press, W. Xu, D. Andruczyk, D. Curreli, and D. N. Ruzic, "Wetting properties of liquid lithium on select fusion relevant surfaces," *Fusion Eng. Des.*, vol. 89, no. 12, pp. 2827–2832, 2014.

[95] "ANSYS® Academic Research, FLUENT Release 15.0."

[96] C. Bachmann, W. Biel, S. Ciattaglia, G. Federici, F. Maviglia, G. Mazzone, G. Ramogida, F. Villone, and N. Taylor, "Initial definition of structural load conditions in DEMO," *Fusion Eng. Des.*, 2017.

[97] G. G. Van Eden, T. W. Morgan, D. U. B. Aussems, M. A. Van Den Berg, K. Bystrov, and M. C. M. Van De Sanden, "Self-Regulated Plasma Heat Flux Mitigation Due to Liquid Sn Vapor Shielding," *Phys. Rev. Lett.*, vol. 116, no. 13, 2016.

[98] P. Fiflis, T. W. Morgan, S. Brons, G. G. Van Eden, M. A. Van Den Berg, W. Xu, D. Curreli, and D. N. Ruzic, "Performance of the lithium metal infused trenches in the magnum PSI linear plasma simulator," *Nucl. Fusion*, vol. 55, no. 11, p. 113004, 2015.